# Progress in theoretical RFP studies: new stimulated helical regimes and similarities with tokamak and stellarator

D. Bonfiglio[1], S. Cappello[1], M. Veranda[1], M. Agostini[1], D. Borgogno[2], L. Chacón[3], D. F. Escande[4,1], A. Fassina[1], P. Franz[1], M. Gobbin[1], D. Grasso[5], P. Piovesan[1], I. Predebon[1], M. E. Puiatti[1], G. Rubino[6], F. Sattin[1] and M. Zuin[1]

[1]Consorzio RFX, 35127 Padova, Italy
[2]Université Cote d'Azur, CNRS, Observatoire de la Cote d'Azur, 06304 Nice, France
[3]Los Alamos National Laboratory, Los Alamos, New Mexico 87545, USA
[4]Aix-Marseille Univ, CNRS, PIIM, UMR 7345, 13013 Marseille, France
[5]Istituto dei Sistemi Complessi-CNR, Politecnico di Torino, 10129 Torino, Italy
[6]ENEA, Fusion and Technologies for Nuclear Safety Department, 00044 Frascati, Italy

*Corresponding Author:* daniele.bonfiglio@igi.cnr.it

**Abstract:**

Recent theoretical studies of the reversed-field pinch (RFP) have demonstrated the possibility of stimulating new quasi-single helicity (QSH) regimes by allowing a small helical deformation of the magnetic boundary. In particular, QSH states based on non-resonant helicities are predicted to be more resilient to magnetic stochasticity induced by secondary modes. This has motivated a series of successful experiments in the RFX-mod device with applied magnetic perturbations (MPs). We present here recent developments in nonlinear MHD modeling of RFP, highlighting aspects which share similarities between the RFP helical regimes, the tokamak sawtoothing and the stellarator. RFP helical configurations are obtained by applying small helical MPs with resonant ($n \geq 7$) and non-resonant ($n < 7$) toroidal periodicities. MPs turn out to be a powerful tool for varying the helical equilibrium properties, like the helical safety factor or the magnetic well profile. The width of the region of conserved magnetic surfaces turns out to be the largest for the non-resonant case. By using a method to compute Lagrangian Coherent Structures, barriers to the diffusion of magnetic field lines are diagnosed in the weakly stochastic region surrounding the conserved helical core in numerical QSH states, providing a new tool for the study of Internal Transport Barriers formation at the transition to helical regimes in RFP experiments. Similar to the tokamak configuration, the sawtoothing dynamics of RFP plasmas is mitigated with the application of helical MPs. As for the edge region, the RFP is characterized by $m = 0$ island chains at the $q = 0$ reversal surface, which play a role similar to edge islands in tokamak and stellarator plasmas.

# 1 Introduction

Recent theoretical studies of the reversed-field pinch (RFP) have demonstrated the possibility of stimulating quasi-single helicity (QSH) regimes by allowing a small helical deformation of the magnetic boundary with helicity close to the "spontaneous" self-organized one [1, 2]. Such small helical magnetic perturbations (MP) can shape the plasma column with their helical twist, increase the level of magnetic order and induce barriers to the transport. Furthermore it is observed that regimes based on non-resonant helicities are more resilient to magnetic stochasticity induced by secondary modes [2]. These theoretical predictions motivated a series of experiments, which have been successfully accomplished in the RFX-mod device: external magnetic perturbations have been demonstrated to trigger helical self-organization within a range of preferred helicities, both resonant and non-resonant. In particular, non-resonant $n = 6$ helical states (built upon actively controlled Resistive Wall Modes) show indications of a broad hot helical core.
In this work we will describe such new RFP states and draw some analogies with helical states observed in other magnetic configurations for magnetic fusion. We will begin by describing the helical RFP in terms of MHD dynamics, magnetic equilibrium and topological properties. The properties of the weakly chaotic states observed are investigated by using new techniques, such as "ridges identification", to detect barriers to the transport of magnetic field lines [3]. Then we discuss the effect of sawtooth mitigation by MPs observed in both RFP and tokamak configurations. Finally, we mention recent analyses highlighting similarities of the helical RFP with the tokamak and the stellarator [4] regarding the edge topological properties in the presence of 3D magnetic fields.

# 2 Numerical tools

The results presented in this work are obtained in the framework of 3D nonlinear MHD model. The model combines Faraday law, a momentum equation, an energy equation and the single fluid resistive Ohm's law to evolve the magnetic field $\boldsymbol{B}$, velocity $\boldsymbol{v}$ and temperature $T$ in time $t$ (see [5] for the model equations). Stationary uniform pressure and plasma density are assumed. With these assumptions, one gets the so-called visco-resistive approximation, a model with two dimensionless parameters: $\eta$ (resistivity) and $\nu$ (viscosity). The numerical implementation of such model is provided by either the SpeCyl code in cylindrical approximation [6] or the PIXIE3D [7] code in toroidal geometry (and extended MHD). Such codes were numerically verified against each other with excellent results [5]. In their common limits of application, an excellent agreement was demonstrated in several fusion-relevant cases. The numerical simulation setup depends on the specific magnetic configuration (RFP, tokamak, stellarator), and we refer the reader to [4] for the details. In the following sections, we focus on the helical magnetic boundary conditions (so-called MPs) employed, which are a key element in this study. The MP helical twist is defined by its toroidal wave number $n_{MP}$ with poloidal wave number $m = 1$, and its amplitude, measured as MP%$= b_r(a)/B(a)$%.

# 3 Stimulated non-resonant and resonant helical RFP regimes

In this section, we show how a small seed helical magnetic perturbation at the edge can steer the global process of RFP helical self-organization towards previously unobserved states, shaping the plasma column with the chosen seed helical periodicity. Examples of magnetic field dynamics in the new regimes are shown in fig. 1. Three stimulated helical configurations with $n = 6$, then with $n = 7$ and $n = 8$ toroidal periodicity are obtained by applying the corresponding seed MP on top of a sawtoothing RFP with central safety factor $q_0 \simeq 1/7$ [1]. Such helical states correspond to the first non-resonant, first and second resonant kink-tearing modes, respectively. Looking at the dynamical evolution of the main MHD modes, it is possible to notice that the mode with the same helicity as the MPs quickly becomes the dominant one and tames the intensity of the others, thus creating a quasi-helical state: this is true not only at the edge but also in the core, as we will see in sec. 4. We find out that the plasma responds to both non-resonant and resonant MPs. The plasma response is the largest for helicities close to the most unstable MHD modes ($n = 7, 8$ in our simulations setup). In the next section, we will focus on a more precise characterization of such states, considering first the helical part of the field only and then the fully 3D one.

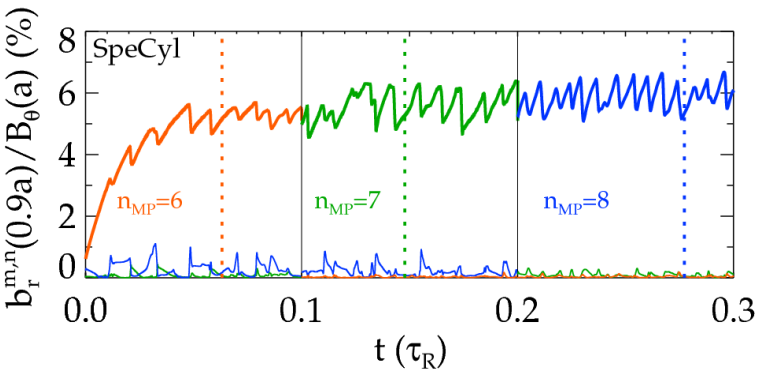


*Figure 1: Small seed MPs can shape the plasma column with their helicity. We show the temporal evolution of the dominant m=1 harmonics of the magnetic field. SpeCyl with $\eta = 10^{-6}$, $\nu = 10^{-4}$, $MP\% = 4\%$.*

# 4 Core confinement properties of RFP regimes

The core properties of numerical RFP regimes with different dominant helicities are strongly related to the so-called "helical equilibrium" magnetic field $\boldsymbol{B}_h$. Such field is obtained by retaining only the axisymmetric component of the total magnetic field plus the harmonics with the dominant helicity. In this section, we analyze the magnetic configurations at the three simulation times marked in fig. 1 and chosen because of the comparable amplitude of the dominant helical mode and of secondary perturbations.
Looking at the first row of fig. 2 it is possible to notice that the dominant helicity is the same as the applied edge MP, and that secondary modes can be neglected as a first approximation, which gives the helical field $\boldsymbol{B}_h$. From such helical equilibrium it is possible to

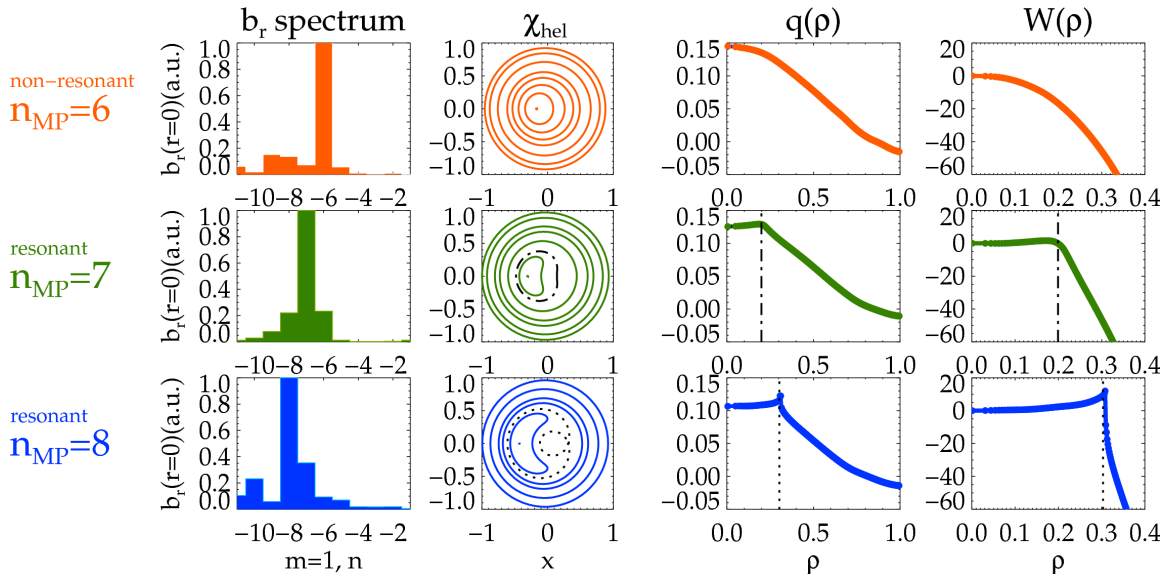


*Figure 2: Helical equilibrium features of stimulated RFP regimes. First column: intensity of the most relevant MHD modes at the snapshots highlighted in figure 1. Second column: helical flux surfaces. Third column: safety factor profile. Fourth column: magnetic well profile.*

define a helical flux function $\chi$ such that $\nabla\chi \cdot \boldsymbol{B}_h = 0$, an effective radius $\rho = \sqrt{\frac{\chi-\chi_{\min}}{\chi_{\max}-\chi_{\min}}}$ and a helical safety factor $q(\rho) = \frac{d\Psi_{tor}}{d\Psi_{pol}}$, namely the number of toroidal turns that field lines perform for one poloidal turn around the *helical magnetic axis*. One can notice that the shape of helical flux surfaces, i.e. surfaces of constant $\chi$ plotted in the second column, varies from almost circular helically displaced surfaces for the non-resonant case to bean-shaped surfaces for the resonant ones. Correspondingly, the safety factor profile decreases monotonically for the non-resonant case, whereas a region of flat or reversed magnetic shear appears in the core for resonant configurations [9, 8], similarly to what is obtained in experimental reconstructions [8]. The case with $n = 8$ dominant helicity is characterized by the presence of a magnetic separatrix. Such a surface acts as a seed for the onset of magnetic chaos, see [10]. In the case with $n = 7$, the separatrix has been expelled by a dynamical transition that changes the topology of the flux surfaces from a double-magnetic axis to a single-magnetic axis, but still its ghost can be noticed corresponding to the beginning of a reversed-shear region. In the $n = 6$ case, the non-resonant nature of the dominant MHD mode avoids from the beginning the formation of a separatrix surface. Another useful quantity in determining the stability of a given configuration is the magnetic well, defined as $W(\rho) = 100[U(0) - U(\rho)]/U(0)$, where $U(\rho) = \frac{dV(\rho)}{d\psi_{tor}(\rho)}$ is the specific volume of a given magnetic surface. This is a key parameter for the stability of pressure-driven modes, mostly used in stellarator research [11]. A stabilizing effect is present where $W'(\rho) > 0$. Resonant helical states are characterized by a positive magnetic well inside the core shear reversal region, whereas the core magnetic well is negative in the non-resonant $n = 6$ case.

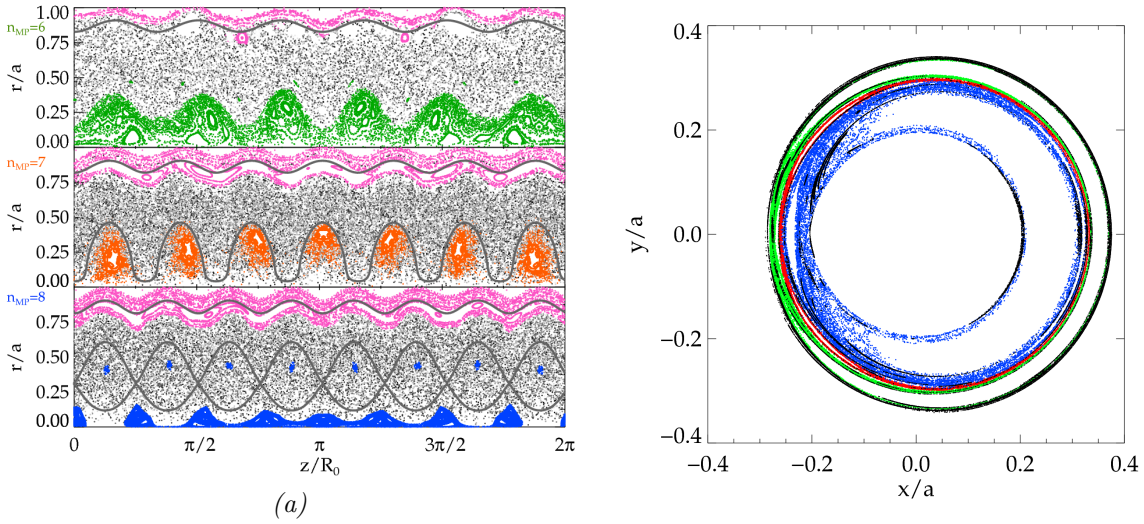


*(a)* *(b)*

*Figure 3:* ***a)*** *Poincaré plots in the r-z plane, corresponding to the three snapshots highlighted in figure 1. Secondary perturbations are divided by two to evidence more the presence of conserved structures. The gray contour lines are the helical flux surfaces at the maximum values of $q(\rho)$ and at $q(\rho) = 0$.* ***b)*** *Ridges (in purple) computed for the simulation described in [3]. Distinct sets of field lines (initialized at the colored dots) do not leak through ridges, for a finite time.*

When secondary MHD modes are taken into account, a magnetic topology characterized by a conserved helical core enclosed by a stochastic region is typically observed. The width of the core-conserved region turns out to be the largest for the non-resonant configuration [2], as can be seen in figure 3a. This property is observed during all the dynamical evolution of the MHD modes, together with the fact that in the non-resonant case the area of core conserved magnetic surfaces encloses the magnetic axis. The observed reduced stochasticity provides the main rationale for pursuing non-resonant helical RFP states as a path towards improved confinement. Indeed, RFX-mod experiments show that the best QSH regimes obtained with a $n = 6$ dominant mode are endowed with a hot helical core, which can be larger than the spontaneous $n = 7$ QSH states [2]. A detailed analysis in terms of confinement is still in progress and will likely need additional data. Generally speaking, confining cantori can be present in the region of stochastic magnetic field [12]. Such cantori have been diagnosed in numerical helical RFP states as Lagrangian Coherent Structures, using a method applied for the first time to magnetic confinement configurations [3]. We determine the map of Finite Time Lyapunov Exponents for the magnetic field lines and identify coherent structures with its "ridges". Figure 3b shows that ridges (indicated by purple lines) act as partial barriers to the transport of magnetic field lines. Field lines starting on the opposite sides of a ridge take a finite time before crossing it. Such confining structures cannot be easily located by simpler diagnosis methods like Poincaré plots.

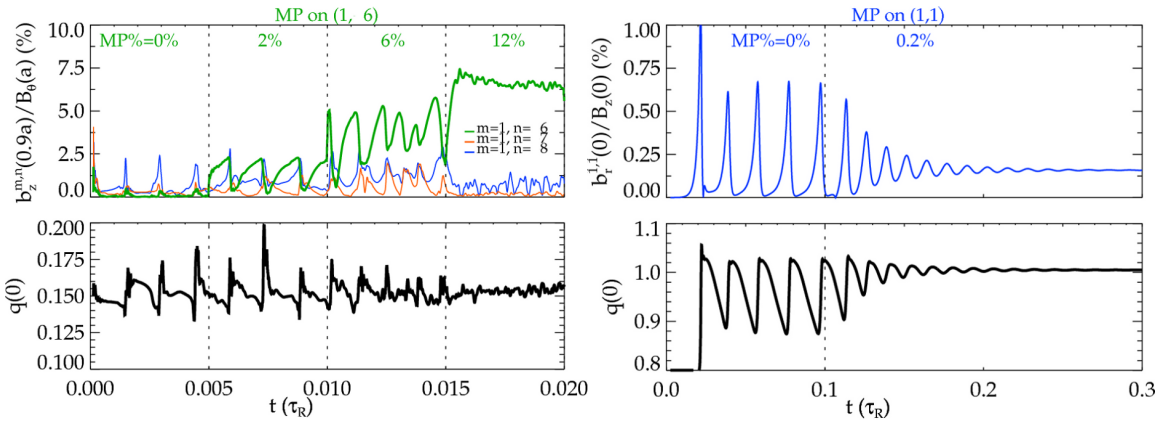


*Figure 4: Effect of MPs on the sawtooth activity in RFP (left) and tokamak (right). On the top we plot the time behaviour of the most important MHD modes while on the bottom the central safety factor value.*

# 5 Sawtooth mitigation with magnetic perturbations in RFP and tokamak

We now discuss the mitigation effect of MPs on the magnetic field oscillations observed both in RFP and tokamak configurations. In numerical RFP modeling, the application of helical magnetic perturbations affects the quasi-periodic sawtoothing dynamics of the configuration: when the amplitude of the helical magnetic perturbation applied in numerical RFP modeling is increased, the sawtooth cycles become more frequent and less intense. Eventually, sawtooth-like oscillations completely disappear and a stationary QSH regime is obtained [4]. The left column of figure 4 shows an example of this behaviour: after MPs are turned on (with $MP\% = 2\%$), the stimulated mode emerges, then it becomes the dominant one (with $MP\% = 6\%$), and a nearly stationary regime is eventually obtained with $MP\% = 12\%$. A qualitatively similar phenomenology is observed in tokamak modeling as well, as can be seen in the right column of fig. 4. In nonlinear MHD simulations of tokamak configurations with initial $q_0 < 1$, sawtooth oscillations associated with the $m = 1$, $n = 1$ internal kink mode are mitigated and possibly replaced by a stationary helical core with the application of $n = 1$ magnetic perturbations [4]. The effect on sawteeth can be obtained with both $m = 1$ helical magnetic perturbations, which directly couple with the core $1, 1$ harmonic, or with a dominantly $m = 2$ perturbation through toroidal coupling. This is observed in both circular and D-shaped tokamak simulations. The above numerical findings show qualitative agreement with experimental observations. In fact, sawtooth mitigation via applied magnetic perturbation has been experimentally demonstrated in RFX-mod (in both RFP and tokamak configurations) and more recently in DIII-D tokamak plasmas [13]. Other fundamental physical processes observed in both RFP and tokamak simulations and experiments are the formation of current sheets during magnetic relaxation events [14, 15] and the MHD dynamo effect due to the helical displacement of magnetic surfaces [16, 17, 18, 19, 20].

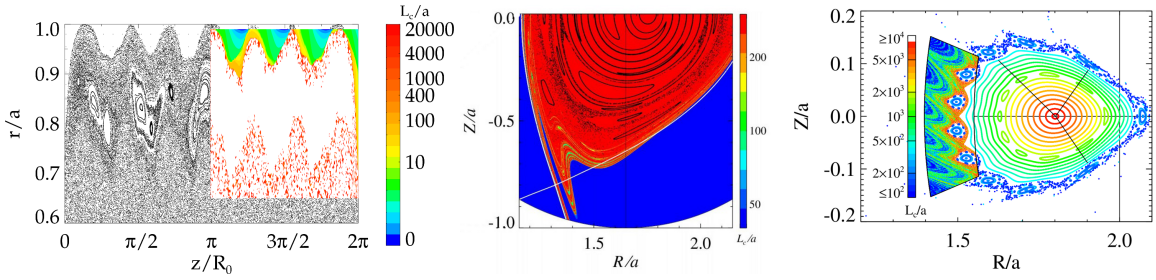


*Figure 5: Edge magnetic topology and connection length to the wall for RFP, tokamak and stellarators configurations. The RFP case is the same as in fig. 3a.*

# 6 Edge confinement properties of RFP, tokamak and stellarator

As a further example of common physics between RFP, tokamak and stellarator, we now discuss the edge topology in the presence of 3D magnetic fields. As a tool to highlight similarities between the different configurations, we use the connection length of magnetic field lines to the wall, which is extensively employed to characterize edge magnetic structures in fusion devices.
In fig. 5a) we show the edge region of the RFP, where a chain of m=0 islands located at the $q = 0$ reversal surface is present (it can be seen, colored in purple, also in figure 3a). This $m = 0$ island chain plays an important role for edge confinement [21] and could be exploited as part of an island divertor system [22]. Here, we show that $m = 0$ islands act as edge transport barrier in stimulated helical RFP states: where the islands are present $L_c$, is much greater, which implies that magnetic field lines are confined for a longer time. Moreover, we provide a comparison with tokamak and stellarator configurations with edge islands, obtained in PIXIE3D modeling [4]. As for the tokamak, an example of PIXIE3D simulations of a diverted tokamak in toroidal geometry in shown. The use of non-axisymmetric MP for sawtooth mitigation, described in section 5, induces a stochastization of the plasma edge and the formation of homoclinic lobes at the X-points [23]. The magnetic topology of vacuum stellarator fields is analyzed in cylindrical geometry with the SpeCyl code (that reproduces analytical solutions) and also in toroidal geometry with the PIXIE3D code. When the helical symmetry provided by the dominant helical mode is violated, magnetic islands and stochastic layers appear, particularly at the edge, where homoclinic lobes are observed in the connection length plot [24].

# 7 Final remarks

This study describes recent advancements in the study of RFP magnetic-fusion plasmas in the framework of 3D nonlinear visco-resistive MHD. The model has been preliminarily applied to different magnetic configurations, like tokamak and stellarators. In the RFP, a key ingredient is the use of small helical edge magnetic fields, which strongly affect self-organization: we showed that they can stimulate global quasi-helical states with the

chosen helical twist, improve field-lines confinement properties and alleviate the periodic reconnection activity typical of the configuration. This last observation pertains also to the tokamak configurations: small MPs can stimulate stationary helical states, with mitigated sawtoothing activity, in analogy with what is observed in the RFP. The stimulation of helical self-organization by applied MPs thus appears as a common effect in different magnetic configurations. Future studies will employ numerical tools (like the "ridge" technique described here and anisotropic heat transport computations in the PIXIE3D code) to investigate the basic mechanisms, yet unknown, that can influence the formation of barriers to transport in all configurations. The impact on electrostatic mode stability and turbulence of the different helical RFP states will be evaluated [25]. Significant work will also be devoted to the comparison between numerical results and experimental measurements, in particular regarding the dynamics of stimulated RFP regimes and their thermal and transport properties.

# Acknowledgements

A part of this work was carried out using the HELIOS supercomputer system at Computational Simulation Centre of International Fusion Energy Research Centre (IFERC-CSC), Aomori, Japan, under the Broader Approach collaboration between Euratom and Japan, implemented by Fusion for Energy and JAEA. This project has received funding from the European Union's Horizon 2020 research and innovation programme under grant agreement number 633053. The views and opinions expressed herein do not necessarily reflect those of the European Commission.

# References

[1] VERANDA, M. et al., Plasma Phys. Control. Fusion **55** (2013) 074015.
[2] VERANDA, M. et al., (2016), Submitted to Phys. Rev. Lett.
[3] RUBINO, G. et al., Plasma Phys. Control. Fusion **57** (2015) 085004.
[4] BONFIGLIO, D. et al., Plasma Phys. Control. Fusion **57** (2015) 044001.
[5] BONFIGLIO, D. et al., Phys. Plasmas **17** (2010) 082501.
[6] CAPPELLO, S. et al., Nucl. Fusion **36** (1996) 571.
[7] CHACÓN, L., Phys. Plasmas **15** (2008) 056103.
[8] GOBBIN, M. et al., Phys. Rev. Lett. **106** (2011) 025001.
[9] BONFIGLIO, D. et al., Phys. Rev. Lett. **111** (2013) 085002.
[10] ESCANDE, D. F. et al., Phys. Rev. Lett. **85** (2000) 3169.
[11] CASTELLANO, J. et al., Physisc of Plasmas **9** (2002) 713.
[12] MACKAY, R. S. et al., Phys. Rev. Lett. **52** (1984) 697.
[13] PIRON, C. et al., Nuclear Fusion **56** (2016) 106012.
[14] CAPPELLO, S., Plasma Phys. Control. Fusion **46** (2004) B313.
[15] ZUIN, M. et al., Overview of the RFX-mod fusion science activity, in *this conference*, 2016.
[16] BONFIGLIO, D. et al., Phys. Rev. Lett. **94** (2005) 145001.
[17] CAPPELLO, S. et al., Phys. Plasmas **13** (2006) 056102.
[18] CAPPELLO, S. et al., Nucl. Fusion **51** (2011) 103012.
[19] JARDIN, S. C. et al., Phys. Rev. Lett. **115** (2015) 215001.
[20] PIOVESAN, P. et al., Role of MHD dynamo in the formation of 3d equilibria in fusion plasmas, in *this conference*, 2016.
[21] SPIZZO, G. et al., Phys. Rev. Lett. **96** (2006) 025001.
[22] MARTINES, E. et al., Nucl. Fusion **50** (2010) 035014.
[23] PUNJABI, A. et al., Phys. Letters A **378** (2014) 2410.
[24] BONFIGLIO, D. et al., 3D MHD simulations of stellarator plasmas with the PIXIE3D and SPECYL codes, in *20th International Stellarator-Heliotron Workshop*, 2015.
[25] PREDEBON, I. et al., Phys. Plasmas **22** (2015) 052308.